

Spin Hamiltonian of Hyperkagome $\text{Na}_4\text{Ir}_3\text{O}_8$

T. Micklitz

*Dahlem Center for Complex Quantum Systems and Institut für Theoretische Physik,
Freie Universität Berlin, 14195 Berlin, Germany*

M. R. Norman

Materials Science Division, Argonne National Laboratory, Argonne, Illinois 60439

(Dated: February 14, 2022)

We derive the spin Hamiltonian for the quantum spin liquid $\text{Na}_4\text{Ir}_3\text{O}_8$, and then estimate the direct and superexchange contributions between near neighbor iridium ions using a tight binding parametrization of the electronic structure. We find a magnitude of the exchange interaction comparable to experiment for a reasonable value of the on-site Coulomb repulsion. For one of the two tight binding parametrizations we have studied, the direct exchange term, which is isotropic, dominates the total exchange. This provides support for those theories proposed to describe this novel quantum spin liquid that assume an isotropic Heisenberg model.

PACS numbers: 75.10.Dg, 75.30.Et, 75.50.Ee

I. INTRODUCTION

$\text{Na}_4\text{Ir}_3\text{O}_8$ has captured much attention since its discovery.^{1,2} This insulator exhibits a large Curie Weiss temperature (650 K), yet does not magnetically order down to the lowest measured temperature. The reason for this is thought to be due to the strongly frustrated nature of the iridium lattice, which forms a hyperkagome network composed of corner sharing triangles (the hyperkagome lattice being formed by replacing one of the four Ir sites in a pyrochlore lattice by a Na ion). Most models that have been proposed to describe this material assume an isotropic Heisenberg model with an effective spin of $1/2$. This is somewhat of a surprise, given the distorted nature of the lattice and the strong spin-orbit coupling of the iridium ions. These issues have been discussed in depth in Ref. 3.

In a previous paper,⁴ we have calculated the exchange constants based on a particular tight binding parametrization of the electronic structure, and found that the resulting spin Hamiltonian should be highly anisotropic. In the present paper, we revisit this issue by considering a more general tight binding parametrization. We now include the residual crystal field splittings of the Ir 5d orbitals due to the octahedral distortions, and find that this corrects a major deficiency of the previous fit, which was an anomalously large value for the t_{dd}^δ hopping. As a result, the more general parametrization leads to the exchange interaction being dominated by the direct exchange between Ir ions, and as a consequence, we find an approximately isotropic Heisenberg model. We also find the observed magnitude of the exchange for a reasonable value of the Coulomb repulsion.

In Section II, we provide a microscopic derivation of the exchange Hamiltonian, finding a few differences from previously published results. In Section III, we describe the tight binding parametrizations of the electronic structure, and then in Section IV, the resulting exchange constants as a function of the Coulomb repulsion. In Section

V, we summarize our findings.

II. EXCHANGE COUPLINGS

In $\text{Na}_4\text{Ir}_3\text{O}_8$, the t_{2g} 5d manifold contains one hole per iridium site (the e_g levels are empty), and the oxygen 2p levels are filled.^{3,4} This single hole sits in a half-filled doublet level due to spin-orbit coupling, thus motivating an effective $S=1/2$ exchange model. This picture, which is supported by our electronic structure calculations, can be exploited to calculate the exchange couplings following Ref. 3.

A. Microscopic Hamiltonian

In our own derivation, we exploit the work of Refs. 5,6, which calculated the exchange couplings for cuprates in the presence of spin-orbit coupling, following the earlier work of Koshibae *et al.*⁷ referred to in Ref. 3. We want to derive the exchange couplings generated to fourth order in the hopping of Ir holes in the t_{2g} complex. Hopping can be direct between the Ir^{4+} ions or via the p-orbitals of the O^{2-} ions. We denote by $\epsilon_{1,2,3}^d$ the Kramers-degenerate energy levels of the t_{2g} complex with $\epsilon_3^d > \epsilon_1^d, \epsilon_2^d$. These splittings are mostly due to the spin-orbit coupling, which acts to form a lower quartet and an upper doublet, but there is a contribution as well from residual crystal field splittings resulting from the low site symmetry of the iridium ion (noting that the space group is cubic).^{3,4} The vacuum state is denoted as $|\Omega\rangle$ where all three levels are fully occupied. The ground state is then generated by linear combinations of the form

$$|\phi_0\rangle = \text{span}\{c_{i3\uparrow}^\dagger|\Omega\rangle, c_{i3\downarrow}^\dagger|\Omega\rangle\} \quad (1)$$

where \uparrow, \downarrow characterizes the Kramers degenerate states, i is the site index, and c^\dagger is the creation operator for a

hole in the t_{2g} complex. According to the Goodenough-Kanamori rules, the strongest contribution to the exchange coupling results from two half-occupied orbitals, so we may focus only on the hopping between the ϵ_3^d orbitals. The Hamiltonian acting on the ground state is then

$$H = H_0 + H_{\text{hop}} \quad (2)$$

with on-site Hamiltonian

$$H_0 = \sum_{im\sigma} \epsilon_m^d c_{im\sigma}^\dagger c_{im\sigma} + \frac{U_d}{2} \sum_{imn\sigma\sigma'} c_{im\sigma}^\dagger c_{in\sigma'}^\dagger c_{in\sigma'} c_{im\sigma} \\ + \sum_{ka\sigma} \epsilon_{ka}^p p_{ka\sigma}^\dagger p_{ka\sigma} + \frac{U_p}{2} \sum_{kab\sigma\sigma'} p_{ka\sigma}^\dagger p_{kb\sigma'}^\dagger p_{kb\sigma'} p_{ka\sigma} \quad (3)$$

where c^\dagger (c) and p^\dagger (p) are creation (annihilation) operators for holes. Indices i and k describe sites of the Ir ion and its nearest-neighbor O ions, m, n and a, b denote the Ir t_{2g} and O p levels, and σ, σ' are spin indices. The relevant hopping between nearest neighbor Ir and O sites is

$$H_{\text{hop}} = \sum_{ij\sigma\sigma'} (t_{33}^{ij})_{\sigma\sigma'} c_{i3\sigma}^\dagger c_{j3\sigma'} \\ + \sum_{ika\sigma\sigma'} \left((t_{a3}^{ki})_{\sigma\sigma'} p_{ka\sigma}^\dagger c_{i3\sigma'} + \text{h.c.} \right) \quad (4)$$

where the spin dependent matrix elements for hopping between Ir, and Ir and O ions, are

$$(t_{33}^{ij})_{\sigma\sigma'} = \tilde{t}_{33}^{ij} \delta_{\sigma\sigma'} + \mathbf{C}_{33}^{ij} \cdot \sigma_{\sigma\sigma'} \quad (5)$$

$$(t_{a3}^{ki})_{\sigma\sigma'} = \tilde{t}_{a3}^{ki} \delta_{\sigma\sigma'} + \mathbf{C}_{a3}^{ki} \cdot \sigma_{\sigma\sigma'} \quad (6)$$

Note that we use a formulation in terms of holes. But to compare with the results of Ref. 3, we will insert for the energies of virtual states that of the electrons and not the holes.

B. Exchange couplings from perturbation theory

The Kramers degenerate ground state is split due to virtual hopping processes. An effective spin Hamiltonian H_S can be derived from perturbation theory in H_{hop} . Accounting only for interactions between neighboring spins it is of the general form

$$H_S = \sum_{\langle ij \rangle} \mathcal{H}_{i,j} \quad (7)$$

Here $\langle ij \rangle$ indicates a sum over nearest neighbor sites and

$$\mathcal{H}_{i,j} = \sum_{pq} J_{pq}(i, j) S_p(i) S_q(j) \quad (8)$$

with spin-1/2 operators \mathbf{S} ($p, q = x, y, z$). In what follows we want to derive expressions for $J_{pq}(i, j)$ up to fourth

order in the hopping. For this it is convenient to introduce

$$T_{ji}^{dd} = \sum_{\sigma\sigma'} (t_{33}^{ji})_{\sigma\sigma'} c_{j3\sigma}^\dagger c_{i3\sigma'} \quad (9)$$

$$T_{ki}^{pd} = \sum_{a\sigma\sigma'} (t_{a3}^{ki})_{\sigma\sigma'} p_{ka\sigma}^\dagger c_{i3\sigma'} \quad (10)$$

$$(T_{ik}^{pd})^\dagger = \sum_{a\sigma\sigma'} (t_{3a}^{ik})_{\sigma\sigma'} c_{i3\sigma}^\dagger p_{ka\sigma'} \quad (11)$$

so that

$$H_{\text{hop}} = \sum_{ji} T_{ji}^{dd} + \sum_{ki} \left(T_{ki}^{pd} + (T_{ik}^{pd})^\dagger \right) \quad (12)$$

The energy of the ground state $|\phi_0\rangle$ is set to zero.

1. Direct exchange

The lowest order contribution results from direct hopping between Ir ions. There are two contributions resulting from the back and forth hopping of holes on Ir sites i and j , respectively. Both processes give identical contributions, so we can restrict ourselves to the hopping of a hole at site i and multiply its contribution by a factor of two,

$$\mathcal{H}_{i,j}^{(2)} = -2 \langle \phi_0 | T_{ij}^{dd} \frac{1}{H_0} T_{ji}^{dd} | \phi_0 \rangle \quad (13)$$

As mentioned above, we want to compare with the findings of Ref. 3 and therefore we give the energy of the intermediate state with two holes on Ir site j in terms of the electron's energy. The latter is $-4U_d + 5U_d = U_d$ and results from the difference in reduced (increased) Coulomb interaction on the site where a hole is inserted (removed). Inserting T_{ji}^{dd} from Eq. 9 we get

$$\mathcal{H}_{i,j}^{(2)} = -\frac{2}{U_d} \sum_{\sigma_1 \sigma_2 \sigma_3 \sigma_4} (t_{33}^{ij})_{\sigma_4 \sigma_3} (t_{33}^{ji})_{\sigma_2 \sigma_1} \\ \langle \phi_0 | c_{i3\sigma_4}^\dagger c_{j3\sigma_3} c_{j3\sigma_2}^\dagger c_{i3\sigma_1} | \phi_0 \rangle \quad (14)$$

We now employ the identity (for notational convenience we suppress the unit matrix in $\frac{1}{2}\mathbb{1}$)

$$c_{i3\sigma_1}^\dagger c_{i3\sigma_2} = \left(\frac{1}{2} + \mathbf{S}_i \cdot \sigma \right)_{\sigma_2 \sigma_1} \quad (15)$$

to rewrite this as

$$\mathcal{H}_{i,j}^{(2)} = \frac{2}{U_d} \text{tr} \left(t_{33}^{ij} \left(\frac{1}{2} + \mathbf{S}_j \cdot \sigma \right) t_{33}^{ji} \left(\frac{1}{2} + \mathbf{S}_i \cdot \sigma \right) \right) \quad (16)$$

where the trace is over spin-indices and we neglected a quadratic term cc^\dagger which does not contribute to the effective spin Hamiltonian in Eq. 8. Terms involving the factor 1/2 lead to contributions which also do not contribute to Eq. 8. Neglecting these we find

$$\mathcal{H}_{i,j}^{(2)} = \frac{2}{U_d} \text{tr} \left(t_{33}^{ij} (\mathbf{S}_j \cdot \sigma) t_{33}^{ji} (\mathbf{S}_i \cdot \sigma) \right) \quad (17)$$

This expression is a factor of two larger than that quoted in Ref. 3.

2. Superechange via oxygen

We now turn to processes involving intermediate oxygen and states arising from fourth order hopping. Let us start with two observations. First, only those processes where the hole hops from one Ir via the O to a different Ir give spin dependent contributions, i.e. processes where the hole hops to O and then returns to the same Ir it started from do not contribute to Eq. 8 and will be neglected in the following. Second, following Ref. 6, we notice that there are two qualitatively different processes in which fourth order hopping contributes to Eq. 8. In the ‘consecutive channel’ (cc) a hole hops from an Ir ion to the O, then to the second Ir, and finally back to the first Ir via the same or a different O. In this channel there are two holes on an Ir ion in the intermediate state. The consecutive channel cc gives an identical contribution as the direct term, however with an effective hopping amplitude $t_{33}^{ij} \rightarrow \tau_{33}^{ij}$. In the second ‘simultaneous channel’ (sc) a hole hops from one of the Ir ions to the O, and then a second hole hops from the second Ir to the same or a different O. Afterwards the holes return to the Ir, i.e. back to the ground state in which one hole occupies each Ir. In this second channel, two holes simultaneously occupy O as intermediate states.

a. Consecutive channel cc: Let us first turn to contributions from the consecutive channel (cc) and look at a hole at Ir site i . Hopping of the hole from site i to j via an O ion at site k results in a state $|\phi_{2j}^{cc}\rangle$ with two holes occupying t_{2g} levels of Ir at site j and no hole on Ir site i ,

$$H_0|\phi_{2j}^{cc}\rangle = (T_{jk}^{pd})^\dagger \frac{1}{H_0} T_{ki}^{pd} |\phi_0\rangle \quad (18)$$

The (electron) energy of the intermediate state after the first hop is a sum of four contributions. Removing the hole from the t_{2g} level and inserting the hole in the a -level of the O ion at site k gives $\epsilon_3^d - \epsilon_{ka}^p$ for the on-site energies and $5(U_d - U_p)$ from the increased and reduced Coulomb interaction between the electrons on Ir and O ions, respectively. That is, the energy of the intermediate state after the first hop is

$$\epsilon_{ka}^{pd} = \epsilon_3^d - \epsilon_{ka}^p + 5(U_d - U_p) \quad (19)$$

Inserting Eq. 10 then gives

$$\begin{aligned} H_0|\phi_{2j}^{cc}\rangle &= \sum_{ak\sigma_1\sigma_2\sigma_3} \frac{1}{\epsilon_{pd}^{pd}} (t_{3a}^{jk})_{\sigma_3\sigma_2} (t_{a3}^{ki})_{\sigma_2\sigma_1} \\ &\quad \times c_{j3\sigma_3}^\dagger p_{ka\sigma_2} p_{ka\sigma_2}^\dagger c_{i3\sigma_1} |\phi_0\rangle \\ &= \sum_{ak\sigma_1\sigma_2\sigma_3} \frac{1}{\epsilon_{pd}^{pd}} (t_{3a}^{jk})_{\sigma_3\sigma_2} (t_{a3}^{ki})_{\sigma_2\sigma_1} c_{j3\sigma_3}^\dagger c_{i3\sigma_1} |\phi_0\rangle \end{aligned} \quad (20)$$

Introducing the effective hopping between Ir sites

$$\tau_{33}^{ji} = \sum_{ak} \frac{t_{3a}^{jk} t_{a3}^{ki}}{\epsilon_{ka}^{pd}} \quad (21)$$

which is a matrix in spin space (summation over intermediate spins is implicit), this is rewritten as

$$H_0|\phi_{2j}^{cc}\rangle = \sum_{\sigma_1\sigma_2} (\tau_{33}^{ji})_{\sigma_2\sigma_1} c_{j3\sigma_2}^\dagger c_{i3\sigma_1} |\phi_0\rangle \quad (22)$$

Eq. 22 corresponds to the intermediate state $T_{ji}^{dd}|\phi_0\rangle$ in the direct exchange hole pathway Eq. 13 with the hopping matrix elements τ_{33}^{ji} . Therefore division by the (electron) energy U_d of the intermediate state Eq. 22 and application of the second hop which returns the hole to Ir site i , we find

$$\mathcal{H}_{i,j}^{(4cc)} = \frac{2}{U_d} \text{tr} \left(\tau_{33}^{ij} (\mathbf{S}_j \cdot \boldsymbol{\sigma}) \tau_{33}^{ji} (\mathbf{S}_i \cdot \boldsymbol{\sigma}) \right) \quad (23)$$

where the factor of two accounts again for the fact that an identical contribution results from a process in which the hole starts at site j .

b. Simultaneous channel sc: In the ‘simultaneous channel’ sc both Ir-holes from sites i and j hop onto O ions in the intermediate state $|\phi_2^{sc}\rangle$. This can occur in a process in which the first hole at site i and then the hole at site j hops, or in the reversed order. The first hop in this process results in the state

$$\begin{aligned} H_0|\phi_1^{sc}\rangle &= \sum_k \left(T_{kj}^{pd} + T_{ki}^{pd} \right) |\phi_0\rangle \\ &= \sum_{ak\sigma_1\sigma_2} \left((t_{a3}^{ki})_{\sigma_2\sigma_1} p_{ka\sigma_2}^\dagger c_{i3\sigma_1} \right. \\ &\quad \left. + (t_{a3}^{kj})_{\sigma_2\sigma_1} p_{ka\sigma_2}^\dagger c_{j3\sigma_1} \right) |\phi_0\rangle \end{aligned} \quad (24)$$

The energy of the intermediate state $|\phi_1^{sc}\rangle$ is again ϵ_{ka}^{pd} in Eq. 19. Adding then the second hole on the same or a different O ion, we obtain the intermediate state $H_0|\phi_2^{sc}\rangle$, i.e.

$$H_0|\phi_2^{sc}\rangle = \sum_{lk} \left(T_{li}^{pd} \frac{1}{H_0} T_{kj}^{pd} + T_{lj}^{pd} \frac{1}{H_0} T_{ki}^{pd} \right) |\phi_0\rangle \quad (25)$$

An explicit expression for this intermediate state is given in Appendix A, and we here only remark that its (electron) energy depends on whether both holes are on the same O ion or not. It has the non-interacting contribution $2\epsilon_3^d - \epsilon_{ka}^p - \epsilon_{lb}^p$, an interaction contribution $5U_d + 5U_d$ from removing holes at Ir sites i and j , and the interaction contribution $-9U_p$ if both holes are on the same O ion and $-10U_p$ in case they are not. This can be summarized as

$$\epsilon_{lb}^{pd} + \epsilon_{ka}^{pd} + U_p \delta_{kl} \quad (26)$$

The return to the ground state can occur again in two ways, i.e., a hole returns first to Ir at site i and then the second returns to site j , or in the reversed order. The overlap of the resulting state with the ground state defines the effective Hamiltonian

$$\mathcal{H}_{i,j}^{(4sc)} = \sum_{nm} \langle \phi_0 | \left((T^{pd})_{in}^\dagger \frac{1}{H_0} (T^{pd})_{jm}^\dagger + (T^{pd})_{jn}^\dagger \frac{1}{H_0} (T^{pd})_{im}^\dagger \right) | \phi_2^{sc} \rangle \quad (27)$$

The calculation of Eq. 27 is identical to the one for cuprates in Refs. 5,6. For completeness we give details in Appendix B, and here merely state that neglecting spin independent contributions, the effective Hamiltonian of interest is

$$\mathcal{H}_{i,j}^{(4sc)} = \sum_{balk} \frac{1}{\epsilon_{lb}^{pd} + \epsilon_{ka}^{pd} + U_p \delta_{kl}} \left(\frac{1}{\epsilon_{lb}^{pd}} + \frac{1}{\epsilon_{ka}^{pd}} \right)^2 \times \text{tr} \left(t_{3b}^{il} t_{b3}^{lj} (\mathbf{S}_j \cdot \sigma) t_{3a}^{jk} t_{a3}^{ki} (\mathbf{S}_i \cdot \sigma) \right) \quad (28)$$

Finally, summing the superexchange contributions from both channels the superexchange contribution is

$$\mathcal{H}_{i,j}^{(4)} = \sum_{balk} g_{ba}^{lk} \text{tr} \left(t_{3b}^{il} t_{b3}^{lj} (\mathbf{S}_j \cdot \sigma) t_{3a}^{jk} t_{a3}^{ki} (\mathbf{S}_i \cdot \sigma) \right) \quad (29)$$

where we introduced

$$g_{ba}^{lk} = \frac{2}{\epsilon_{lb}^{pd} \epsilon_{ka}^{pd} U_d} + \frac{1}{\epsilon_{lb}^{pd} + \epsilon_{ka}^{pd} + U_p \delta_{kl}} \left(\frac{1}{\epsilon_{lb}^{pd}} + \frac{1}{\epsilon_{ka}^{pd}} \right)^2 \quad (30)$$

Note that the expression for g differs from that of Ref. 3. This difference was previously noted in Refs. 5,6,8 in connection with the similar expression in Ref. 7.

C. Exchange Constants

We next want to bring Eq. 17 for the direct exchange into the form

$$\mathcal{H}_{i,j} = J \mathbf{S}_i \cdot \mathbf{S}_j + \mathbf{D}^{ij} \cdot (\mathbf{S}_i \times \mathbf{S}_j) + \mathbf{S}_i \cdot \vec{\Gamma}^{\leftrightarrow ij} \cdot \mathbf{S}_j \quad (31)$$

To this end we insert Eqs. 5 and 6 into Eq. 17

$$\mathcal{H}_{i,j}^{(2)} = \frac{2}{U_d} \text{tr} \left((\tilde{t}_{33}^{ij} + \mathbf{C}_{33}^{ij} \cdot \sigma) (\mathbf{S}_j \cdot \sigma) (\tilde{t}_{33}^{ji} + \mathbf{C}_{33}^{ji} \cdot \sigma) (\mathbf{S}_i \cdot \sigma) \right) \quad (32)$$

We then employ the identity (checked in Appendix B)

$$\begin{aligned} & \frac{1}{2} \text{tr} ((A_1 + \mathbf{B}_1 \cdot \sigma)(\mathbf{S}_i \cdot \sigma)(A_2 + \mathbf{B}_2 \cdot \sigma)(\mathbf{S}_j \cdot \sigma)) \\ &= A_1 A_2 \mathbf{S}_i \cdot \mathbf{S}_j + i (A_2 \mathbf{B}_1 - A_1 \mathbf{B}_2) \cdot (\mathbf{S}_i \times \mathbf{S}_j) \\ &+ \mathbf{S}_i \cdot \left(\vec{\mathbf{B}}_1 \vec{\mathbf{B}}_2 + \vec{\mathbf{B}}_2 \vec{\mathbf{B}}_1 - \mathbf{B}_1 \cdot \mathbf{B}_2 \vec{\mathbb{1}} \right) \cdot \mathbf{S}_j \end{aligned} \quad (33)$$

to find that $\mathcal{H}_{i,j}^{(2)}$ is of the form Eq. 31 with

$$J^{(2)} = \frac{4}{U_d} \tilde{t}_{33}^{ij} \tilde{t}_{33}^{ji} \quad (34)$$

$$\mathbf{D}_{ij}^{(2)} = -\frac{4i}{U_d} \left(\tilde{t}_{33}^{ji} \mathbf{C}_{33}^{ij} - \tilde{t}_{33}^{ij} \mathbf{C}_{33}^{ji} \right) \quad (35)$$

$$\vec{\Gamma}_{ij}^{(2)} = \frac{4}{U_d} \left(\vec{\mathbf{C}}_{33}^{ji} \vec{\mathbf{C}}_{33}^{ij} + \vec{\mathbf{C}}_{33}^{ij} \vec{\mathbf{C}}_{33}^{ji} - \mathbf{C}_{33}^{ij} \cdot \mathbf{C}_{33}^{ji} \vec{\mathbb{1}} \right) \quad (36)$$

To do the same calculation for the superexchange Eq. 29, let us first rewrite products of hopping matrices

$$\begin{aligned} t_{3b}^{il} t_{b3}^{lj} &= (\tilde{t}_{3b}^{il} + \mathbf{C}_{3b}^{il} \cdot \sigma) (\tilde{t}_{b3}^{lj} + \mathbf{C}_{b3}^{lj} \cdot \sigma) \\ &= \tilde{t}_{3b}^{il} \tilde{t}_{b3}^{lj} + \mathbf{C}_{3b}^{il} \cdot \mathbf{C}_{b3}^{lj} \\ &\quad + \left(i(\mathbf{C}_{3b}^{il} \times \mathbf{C}_{b3}^{lj}) + \tilde{t}_{3b}^{il} \mathbf{C}_{b3}^{lj} + \mathbf{C}_{3b}^{il} \tilde{t}_{b3}^{lj} \right) \cdot \sigma \\ &= s_{ij}^{lb} + \mathbf{v}_{ij}^{lb} \cdot \sigma \end{aligned} \quad (37)$$

where in the last line we introduced

$$s_{ij}^{lb} = \tilde{t}_{3b}^{il} \tilde{t}_{b3}^{lj} + \mathbf{C}_{3b}^{il} \cdot \mathbf{C}_{b3}^{lj} \quad (38)$$

$$\mathbf{v}_{ij}^{lb} = i(\mathbf{C}_{3b}^{il} \times \mathbf{C}_{b3}^{lj}) + \tilde{t}_{3b}^{il} \mathbf{C}_{b3}^{lj} + \mathbf{C}_{3b}^{il} \tilde{t}_{b3}^{lj} \quad (39)$$

We can now apply again Eq. 33 to find

$$\begin{aligned} \mathcal{H}_{i,j}^{(4)} &= \sum_{balk} g_{ba}^{lk} \text{tr} \left((s_{ij}^{lb} + \mathbf{v}_{ij}^{lb} \cdot \sigma) (\mathbf{S}_j \cdot \sigma) \right. \\ &\quad \times (s_{ji}^{ka} + \mathbf{v}_{ji}^{ka} \cdot \sigma) (\mathbf{S}_i \cdot \sigma) \left. \right) \\ &= J \mathbf{S}_i \cdot \mathbf{S}_j + \mathbf{D}^{ij} \cdot (\mathbf{S}_i \times \mathbf{S}_j) + \mathbf{S}_i \cdot \vec{\Gamma}^{\leftrightarrow ij} \cdot \mathbf{S}_j \end{aligned} \quad (40)$$

with

$$J^{(4)} = 2 \sum_{balk} s_{ij}^{lb} g_{ba}^{lk} s_{ji}^{ka} \quad (41)$$

$$\mathbf{D}_{ij}^{(4)} = -2i \sum_{balk} (\mathbf{v}_{ij}^{lb} g_{ba}^{lk} s_{ji}^{ka} - s_{ij}^{lb} g_{ba}^{lk} \mathbf{v}_{ji}^{ka}) \quad (42)$$

$$\vec{\Gamma}_{ij}^{(4)} = 2 \sum_{balk} \left(\vec{\mathbf{v}}_{ij}^{lb} g_{ba}^{lk} \vec{\mathbf{v}}_{ji}^{ka} + \vec{\mathbf{v}}_{ji}^{lb} g_{ba}^{lk} \vec{\mathbf{v}}_{ij}^{ka} - \mathbf{v}_{ij}^{lb} g_{ba}^{lk} \cdot \mathbf{v}_{ji}^{ka} \vec{\mathbb{1}} \right) \quad (43)$$

and g_{ba}^{lk} given in Eq. 30.

III. TIGHT BINDING PARAMETRIZATION

In Ref. 4, we performed local density approximation calculations for the electronic structure of $\text{Na}_4\text{Ir}_3\text{O}_8$, and then performed a tight binding fit within a Slater-Koster

formalism. To understand the tight binding fit, we need to step back and take a look at the electronic structure of this material.^{3,4} $\text{Na}_4\text{Ir}_3\text{O}_8$ is composed of IrO_6 octahedra, and as with many transition metal oxides, these octahedra are distorted, with just a C_2 symmetry axis preserved. Moreover, there are two types of oxygens, with four of the six around an Ir ion being of one type (O2), the other two of the other type (O1). Note that the two O1 ions are not related by an inversion like in cuprates, but are related by a π rotation about the C_2 axis (see Fig. 1). A minimal tight binding model restricted to near neighbors only would then consist of hoppings of Ir to O1, Ir to O2, O1 to O1, O2 to O2, O1 to O2, and Ir to Ir. Because of the distorted nature of the lattice, not all distances between given atom types are the same. To reduce the number of fit parameters, we then assumed a typical inverse fourth power dependence of the hopping integrals with distance for a given atom combination. In practice, this affects only the O to O hoppings, and we note that an inverse fourth power behavior was indeed found for IrO_2 .⁹ The net result is that we need 18 tight binding parameters: energies of t_{2g} ($\epsilon_{t_{2g}}$) and e_g (ϵ_{e_g}) 5d orbitals on Ir, energies of 2p orbitals on O1 and O2 (ϵ_{O1} , ϵ_{O2}) d-d hoppings (t_{dd}^σ , t_{dd}^π , t_{dd}^δ), d-p hoppings (t_{dp}^σ , t_{dp}^π for Ir-O1 and Ir-O2), p-p hoppings (t_{pp}^σ , t_{pp}^π for O1-O1, O2-O2, O1-O2), and the coefficient of the spin orbit splitting for the Ir 5d orbitals, λ (i.e., $\lambda \mathbf{l} \cdot \mathbf{s}$).

These parameters are then used to evaluate the various elements of the secular matrix that generates the eigenvalues.¹⁰ The diagonal elements are simply given by the various on-site energies, and the spin-orbit coupling matrix elements in a crystal field basis compatible with that used in Ref. 10 can be found in Ref. 11. The off-diagonal matrix elements are of the form $t_{ai,bj}(l,m,n)e^{i\mathbf{k} \cdot (\mathbf{r}_j - \mathbf{r}_i)}$ where t is the hopping integral between orbital a on site i and orbital b on site j , and l, m, n are the three direction cosines between the two sites at \mathbf{r}_i and \mathbf{r}_j . In our case, the resulting secular matrix has dimension 312 (there are four formula units in the unit cell, i.e., there are 120 Ir 5d orbitals and 192 O 2p orbitals in the unit cell when spin-orbit is included). In considering off-diagonal elements of the secular matrix, note that each iridium ion is surrounded by six oxygens and four other iridium ions (Fig. 1), and each oxygen is surrounded by twelve other oxygens. Once the secular matrix is set up, then the various tight binding parameters are iteratively adjusted to achieve an optimal fit to the band structure eigenvalues. The function being minimized is a sum of the squares of the differences of the tight binding eigenvalues from the first principles ones of the electronic structure calculation. The minimization was performed using Powell's method.¹² We first fit the calculation without spin-orbit using 42 eigenvalues (the bottom and tops of the O1, O2, and e_g complexes, as well as all 36 bands of the t_{2g} complex) at each of the four symmetry points of the simple cubic Brillouin zone. As an initial start to the minimization, we used previously derived tight binding parameters for IrO_2 ,⁹ scaled (by an assumed inverse

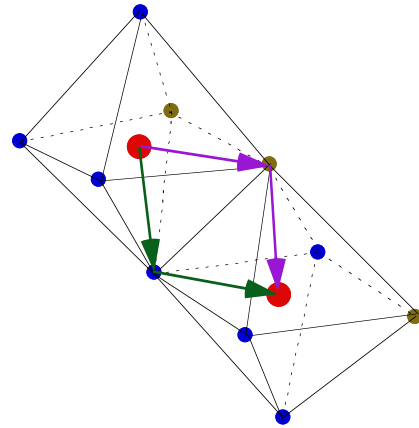


FIG. 1: (Color online) Superexchange pathway between two Ir ions as marked by the arrows. The Ir ions are the large (red) spheres and the oxygen ions the small ones. The lower left (green) pathway is via an O2 (blue) ion, the upper right (purple) pathway via an O1 (brown) ion.

fourth power dependence on distance) to the $\text{Na}_4\text{Ir}_3\text{O}_8$ lattice. The starting values for the on-site energies were estimated from the orbital decomposed density of states of the band calculation. After minimization, the resulting tight binding parameters were then used as input to fitting the calculation with spin-orbit, now involving 78 eigenvalues (the bottom and tops of the O1, O2, and e_g complexes, as well as all 72 bands of the t_{2g} complex), again at the four symmetry points. For the initial start, the spin-orbit coupling parameter, λ , was estimated from the splitting of the $j = 3/2$ and $j = 5/2$ eigenvalues of the band calculation. After minimization, the resulting fit gave a good reproduction of the energy bands, along with the Fermi surface (Figs. 8 and 9 of Ref. 4). This is non-trivial, given the low site symmetry of this lattice, the size of the secular matrix, and the large 18 parameter function space.

This fit, though, does not take into account the residual crystal field splitting of the 5d orbitals due to the distortions of the octahedra. These splittings, although somewhat obscured by hybridization, appear to be present (Fig. 3 of Ref. 4), and could potentially be of importance. Including them increases the number of tight binding parameters to 21 (with two more parameters needed for the t_{2g} manifold and one for the e_g one). A complete description of these splittings are complicated because they involve a number of crystal field potential terms, $V_{20}, V_{21}, V_{22}, V_{40}, V_{41}, V_{42}, V_{43}, V_{44}$, whose coefficients are difficult to estimate from first principles. Rather, we used a simplified approach where we ignore the small coupling between the t_{2g} and e_g orbitals. For a C_2 axis along (1,1,0), the t_{2g} diagonal elements of the secular matrix would be (relative to $\epsilon_{t_{2g}}$) of the form $-2c_1$ for xy , and $+c_1$ for xz and yz , with an off-diagonal matrix element

TABLE I: Tight binding hopping parameters in eV from the 21 parameter fit. The on-site energies are $\epsilon_{O1} = -6.4241$, $\epsilon_{O2} = -3.9141$, $\epsilon_{t_{2g}} = -1.7230$, $\epsilon_{e_g} = 0.6619$, with the spin-orbit coupling $\lambda = 0.5797$. The residual crystal field splittings of the cubic levels on the Ir sites are denoted as c_i ($i = 1, 2, 3$).

	σ	π	δ
Ir-O1	-1.6015	0.8671	
Ir-O2	-2.4604	1.1507	
Ir-Ir	-0.4799	0.0049	0.0521
O1-O1	0.5694	0.0284	
O2-O2	0.4823	-0.3264	
O1-O2	0.6261	0.2560	
	1	2	3
c_i	0.0324	-0.3839	0.2965

$\pm c_3$ between xz and yz , the sign depending on whether the C_2 axis is along $(1,1,0)$ or $(1,-1,0)$. Diagonalization of this sub-matrix leads to two even symmetry states and one odd symmetry state relative to the C_2 axis. We note that this simplified form ignores the smaller off-diagonal matrix element between xy and xz, yz which would couple the two even symmetry states. For the e_g sub-matrix, the diagonal matrix elements (relative to ϵ_{e_g}) are $-2c_2$ for $x^2 - y^2$ and $+2c_2$ for $3z^2 - r^2$. Diagonalization of this sub-matrix leads to one even symmetry and one odd symmetry state. As the C_2 axis is rotated from one iridium site to the next, these t_{2g} and e_g sub-matrices in turn must be rotated (leading to off-diagonal terms between $x^2 - y^2$ and $3z^2 - r^2$).

The resulting 21 parameter tight binding fit had about a 25% smaller RMS error than the 18 parameter one (the band dispersion from the fit is plotted in Fig. 2). On the other hand, the solution space is more complex than in the 18 parameter case, and as a consequence, it is difficult to estimate how well the minimization routine has succeeded in finding an optimal solution. In particular, the c_i parameters (Table I) lead to effective level splittings for the t_{2g} and e_g orbitals that do not seem to correspond well to those indicated by the band structure calculation (Fig. 3 of Ref. 4). Moreover, the Fermi surface is somewhat degraded relative to the one of the 18 parameter fit (Fig. 9 of Ref. 4). On the other hand, the 21 parameter fit corrects a major deficiency of the 18 parameter one, in that t_{dd}^δ , which was anomalously large in the 18 parameter fit (0.1545 eV), is now far more reasonable (0.0521 eV). This, and other differences in the tight binding parameters (comparing Table I with Table II of Ref. 4), turn out to have a qualitative impact on the exchange constants, as we will see in the next Section.

IV. EXCHANGE CONSTANTS

The exchange constants are derived by taking the tight binding parameters discussed in the previous Section and

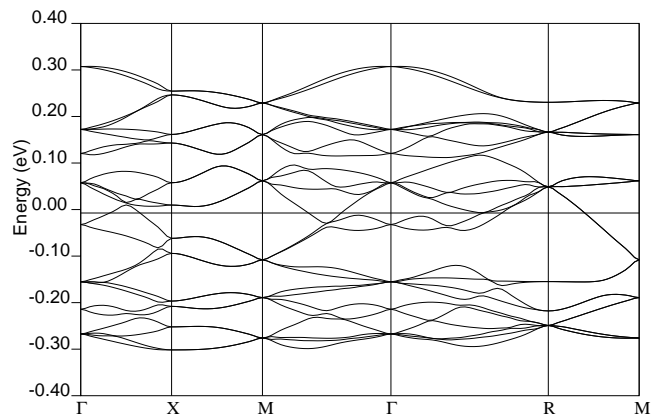


FIG. 2: Energy bands (t_{2g} spin-orbit ‘doublet’) near the Fermi energy (E_F) from the 21 parameter tight binding fit to the electronic structure of $\text{Na}_4\text{Ir}_3\text{O}_8$. The horizontal line marks E_F .

inserting them into the expressions derived in Section II (with $\epsilon_3^d = 0$). We remind that the functional form for the spin Hamiltonian is listed in Eq. 31. As stated previously in Ref. 4, the direct exchange term only contributes to the isotropic term J in Eq. 31; the other terms vanish, even for the distorted lattice. This is a consequence of the fact that the spin-orbit coupling leads to a ‘doublet’ of states around the Fermi energy (the 24 bands shown in Fig. 2) which to a good approximation are formed from linear combinations of xy , xz , and yz orbitals with equal weights. The resulting contribution to J is of the form $4t_d^2/U$ where $t_d = \frac{1}{4}t_{dd}^\sigma + \frac{1}{3}t_{dd}^\pi + \frac{5}{12}t_{dd}^\delta$ (this differs by a factor of two from Ref. 4, as already noted after Eq. 17). On the other hand, the superexchange terms contribute to J , \mathbf{D} and $\mathbf{\Gamma}$. We denote the components of the diagonal contributions to the exchange by $J_i \equiv J + D_i + \Gamma_{ii}$ ($i = x, y, z$). These values are plotted in Fig. 3 as a function of U_d (Coulomb repulsion on the Ir sites) for both sets of tight binding parameters. For the purposes of these plots, U_p (Coulomb repulsion on the O sites) was set to zero.

For the 18 parameter fit, J_x becomes equal to the experimental value of 28 meV¹ for a value of U_d of about 1.1 eV (Fig. 3a). In that context, although the value of U_d is not known for $\text{Na}_4\text{Ir}_3\text{O}_8$, we note that for the related perovskite, Sr_2IrO_4 , the optical gap is 0.5 eV, and it is known from LDA+U simulations that a U_d of about 2 eV is needed to reproduce this gap.¹³ Interestingly, J_y and J_z significantly differ from J_x , indicating that the predicted spin Hamiltonian from this tight binding fit is strongly anisotropic, as we previously remarked.⁴

We can contrast this with the 21 parameter fit, shown in Fig. 3b. J_x reaches the experimental value of 28 meV for a U_d of about 1.5 eV, which is close to the anticipated value of 2 eV. More interestingly, J_y and J_z are close in value to J_x . This indicates a far more isotropic spin Hamiltonian, which is in support of various theo-

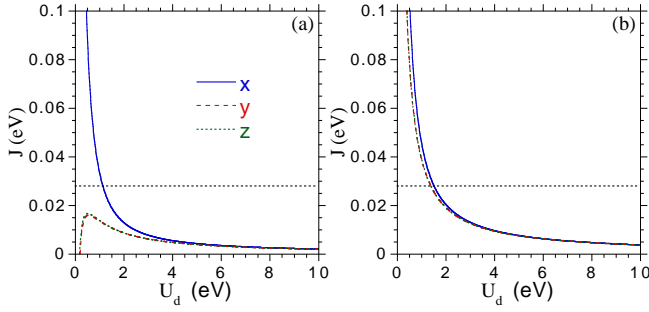


FIG. 3: (Color online) Diagonal elements of the exchange interaction as a function of the on-site repulsion (U_d) on the iridium sites, assuming zero repulsion (U_p) on the oxygen sites; (a) is from the 18 parameter tight binding fit and (b) from the 21 parameter fit. The horizontal dashed line is the experimental value for J .¹

ries for this material. For completeness, we list all the coefficients of the spin Hamiltonian in Table II for the 21 parameter fit with $U_d = 1.5$ eV. We note not only the effective isotropy of J_i , but also the much reduced value of the Dzyaloshinski-Moriya interaction compared to what was previously indicated in Ref. 4. This difference is mainly due to the much smaller value of U_d (0.5 eV) assumed in the previous work. On general grounds, we note the dominance of J_d in Table II compared to the other exchange terms, in particular, the large ratio of J_d to J_s . This is in contrast to the well known case of cuprates, where the superexchange term is dominant. This difference can be attributed to the 90 degree Ir-O-Ir bond present in this material compared to the 180 degree Cu-O-Cu bond found in the cuprates. Other qualitative differences between the 90 and 180 degree cases have been emphasized in the recent work of Jackeli and Khaliullin.¹⁴

Finally, we show in Fig. 4 the dependence of the exchange constants on U_p . Its effect is to cause increased anisotropy. However, this is more pronounced for the 18

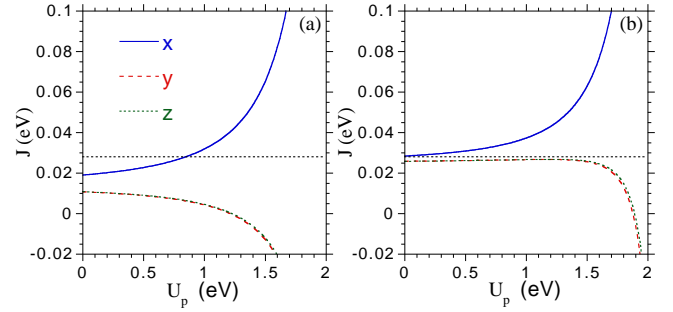


FIG. 4: (Color online) Diagonal elements of the exchange interaction as a function of the on-site repulsion (U_p) on the oxygen sites, with a repulsion (U_d) of 1.5 eV on the iridium sites; (a) is from the 18 parameter tight binding fit and (b) from the 21 parameter fit. The horizontal dashed line is the experimental value for J .¹

parameter fit than the 21 parameter one. At larger values of U_p than those shown in Fig. 4, there are divergences that are associated with zeros of the denominators entering g (Eq. 30). This corresponds to intermediate states that are low in energy, meaning that perturbation theory is no longer valid. Obviously, for very large values of U_p , the superexchange contributions disappear, leaving only the isotropic direct exchange term.

From the above, it is obvious that the exchange constants are very sensitive to the tight binding parametrization, and also the values of the various Coulomb repulsions. We also note that higher order processes are ignored, for instance, sixth order superexchange processes involving additional hoppings between the two O ions connecting two Ir sites which are known to play a role for the honeycomb lattice found in Na_2IrO_3 .¹⁵ Longer range hoppings on the iridium sublattice could also be of importance as well.¹⁶

V. SUMMARY

We have found that an approximately isotropic Heisenberg model can be motivated from a tight binding parametrization of the electronic structure of $\text{Na}_4\text{Ir}_3\text{O}_8$, with the experimental value of J reproduced for a reasonable value of the Coulomb repulsion, U_d . To obtain this result, it was important to account for the residual crystal field splittings of the Ir 5d orbitals due to the octahedral distortions. Our findings are obviously of some importance in regards to models for this quantum spin liquid, since anisotropy acts to stabilize long range magnetic order.³ The large value of the exchange is of much interest, since a large J appears to be associated with the unusual properties of cuprates, including their d-wave superconductivity.¹⁷

TABLE II: Exchange constants in meV from the 21 parameter tight binding fit. The spin Hamiltonian is given in Eq. 31. Quoted are values where Ir site m is along an $(0,1,-1)$ direction relative to Ir site n . D are the Dzyaloshinski-Moriya, and Γ the anisotropic superexchange terms (in the second row for Γ , the jk refer to the parenthesis, xy , etc.). In addition, the direct exchange (isotropic) is $J_d = 24.9$, and the isotropic superexchange term is $J_s = 2.2$. The last row, J_i , is the total exchange for the diagonal components ($J_d + J_s + \Gamma_{ii}$). The assumed value of U_d is 1.5 eV (with U_p assumed to be zero).

$i (jk)$	$x (xy)$	$y (xz)$	$z (yz)$
D_i	3.4	0.4	-0.3
Γ_{ii}	1.3	-1.3	-1.3
Γ_{jk}	0.3	-0.2	-0.0
J_i	28.4	25.8	25.8

Acknowledgments

We thank Gang Chen and Jaejun Yu for discussions. Work at Argonne National Laboratory was supported by

the U.S. DOE, Office of Science, under Contract No. DE-AC02-06CH11357.

Appendix A: Intermediate states in the superexchange pathway

For self-containedness this Appendix provides intermediate steps of the superexchange calculations similar to those found in Ref. 5. The explicit expression for the intermediate state in the simultaneous channel of the superexchange pathway, Eq. 25, is a sum of the two contributions

$$H_0|\phi_2^{sc,a}\rangle = \sum_{lk} T_{lj}^{pd} \frac{1}{H_0} T_{ki}^{pd} |\phi_0\rangle = - \sum_{ba} \sum_{lk} \sum_{\sigma_4 \sigma_3} \sum_{\sigma_2 \sigma_1} \frac{1}{\epsilon_{ka}^{pd}} (t_{b3}^{lj})_{\sigma_4 \sigma_3} (t_{a3}^{ki})_{\sigma_2 \sigma_1} p_{lb\sigma_4}^\dagger p_{ka\sigma_2}^\dagger c_{j3\sigma_3} c_{i3\sigma_1} |\phi_0\rangle \quad (A1)$$

$$H_0|\phi_2^{sc,b}\rangle = \sum_{lk} T_{li}^{pd} \frac{1}{H_0} T_{kj}^{pd} |\phi_0\rangle = - \sum_{ba} \sum_{lk} \sum_{\sigma_4 \sigma_3} \sum_{\sigma_2 \sigma_1} \frac{1}{\epsilon_{ka}^{pd}} (t_{b3}^{li})_{\sigma_4 \sigma_3} (t_{a3}^{kj})_{\sigma_2 \sigma_1} p_{lb\sigma_4}^\dagger p_{ka\sigma_2}^\dagger c_{j3\sigma_3} c_{i3\sigma_1} |\phi_0\rangle \quad (A2)$$

where the minus sign results from exchanging operators p^\dagger and c . Upon relabeling indices $a \leftrightarrow b$, $k \leftrightarrow l$, $\sigma_2 \leftrightarrow \sigma_4$, and $\sigma_1 \leftrightarrow \sigma_3$ we add up both contributions, resulting in the intermediate state

$$H_0|\phi_2^{sc}\rangle = - \sum_{ba} \sum_{lk} \sum_{\sigma_4 \sigma_3} \sum_{\sigma_2 \sigma_1} \left(\frac{1}{\epsilon_{lb}^{pd}} + \frac{1}{\epsilon_{ka}^{pd}} \right) (t_{b3}^{lj})_{\sigma_4 \sigma_3} (t_{a3}^{ki})_{\sigma_2 \sigma_1} p_{lb\sigma_4}^\dagger p_{ka\sigma_2}^\dagger c_{j3\sigma_3} c_{i3\sigma_1} |\phi_0\rangle \quad (A3)$$

and the state $|\phi_2^{sc}\rangle$ has the energy Eq. 26. The return to the ground state can occur in the two processes described in Eq. 27. In the intermediate state $H_0|\phi_{3i}^{sc}\rangle = \sum_m (T^{pd})_{im}^\dagger |\phi_2^{sc}\rangle$ of the first process one hole has returned to site i ,

$$H_0|\phi_{3i}^{sc}\rangle = - \sum_{cba} \sum_{mlk} \sum_{\sigma_6 \sigma_5 \sigma_4 \sigma_3} \sum_{\sigma_2 \sigma_1} \frac{(t_{3c}^{im})_{\sigma_6 \sigma_5} (t_{b3}^{lj})_{\sigma_4 \sigma_3} (t_{a3}^{ki})_{\sigma_2 \sigma_1}}{\epsilon_{lb}^{pd} + \epsilon_{ka}^{pd} + U_p \delta_{kl}} \left(\frac{1}{\epsilon_{lb}^{pd}} + \frac{1}{\epsilon_{ka}^{pd}} \right) c_{i3\sigma_6}^\dagger p_{mc\sigma_5} p_{lb\sigma_4}^\dagger p_{ka\sigma_2}^\dagger c_{j3\sigma_3} c_{i3\sigma_1} |\phi_0\rangle \quad (A4)$$

Using fermion anti-commutation relations and keeping only those contributions that are not annihilated upon acting on the ground state, $p_{mc\sigma_5} p_{lb\sigma_4}^\dagger p_{ka\sigma_2}^\dagger = \delta_{ml} \delta_{bc} \delta_{\sigma_5 \sigma_4} p_{ka\sigma_2}^\dagger - \delta_{km} \delta_{ac} \delta_{\sigma_5 \sigma_2} p_{lb\sigma_4}^\dagger$, which inserted into Eq. A4 shows that $H_0|\phi_{3i}^{sc}\rangle = H_0(|\phi_{3i}^{sc,a}\rangle + |\phi_{3i}^{sc,b}\rangle)$ where

$$H_0|\phi_{3i}^{sc,a}\rangle = \sum_{ba} \sum_{lk} \sum_{\sigma_6 \sigma_4 \sigma_3} \sum_{\sigma_2 \sigma_1} \frac{(t_{3b}^{il})_{\sigma_6 \sigma_4} (t_{b3}^{lj})_{\sigma_4 \sigma_3} (t_{a3}^{ki})_{\sigma_2 \sigma_1}}{\epsilon_{lb}^{pd} + \epsilon_{ka}^{pd} + U_p \delta_{kl}} \left(\frac{1}{\epsilon_{lb}^{pd}} + \frac{1}{\epsilon_{ka}^{pd}} \right) p_{ka\sigma_2}^\dagger c_{i3\sigma_6}^\dagger c_{j3\sigma_3} c_{i3\sigma_1} |\phi_0\rangle \quad (A5)$$

$$H_0|\phi_{3i}^{sc,b}\rangle = - \sum_{ba} \sum_{lk} \sum_{\sigma_6 \sigma_4 \sigma_3} \sum_{\sigma_2 \sigma_1} \frac{(t_{3a}^{ik})_{\sigma_6 \sigma_4} (t_{b3}^{lj})_{\sigma_4 \sigma_3} (t_{a3}^{ki})_{\sigma_2 \sigma_1}}{\epsilon_{lb}^{pd} + \epsilon_{ka}^{pd} + U_p \delta_{kl}} \left(\frac{1}{\epsilon_{lb}^{pd}} + \frac{1}{\epsilon_{ka}^{pd}} \right) p_{lb\sigma_4}^\dagger c_{i3\sigma_6}^\dagger c_{j3\sigma_3} c_{i3\sigma_1} |\phi_0\rangle \quad (A6)$$

States $|\phi_{3i}^{sc,a}\rangle$ and $|\phi_{3i}^{sc,b}\rangle$ have the energies ϵ_{ka}^{pd} and ϵ_{lb}^{pd} , respectively. Acting with a second hopping Hamiltonian the second hole returns to its ground state

$$\sum_m (T^{pd})_{jm}^\dagger |\phi_{3i}^{sc,a}\rangle = \sum_{ba} \sum_{lk} \sum_{\sigma_8 \sigma_6 \sigma_4 \sigma_3} \sum_{\sigma_2 \sigma_1} \frac{(t_{3a}^{jk})_{\sigma_8 \sigma_6} (t_{3b}^{il})_{\sigma_6 \sigma_4} (t_{b3}^{lj})_{\sigma_4 \sigma_3} (t_{a3}^{ki})_{\sigma_2 \sigma_1}}{(\epsilon_{lb}^{pd} + \epsilon_{ka}^{pd} + U_p \delta_{kl}) \epsilon_{ka}^{pd}} \left(\frac{1}{\epsilon_{lb}^{pd}} + \frac{1}{\epsilon_{ka}^{pd}} \right) c_{j3\sigma_8}^\dagger c_{i3\sigma_6}^\dagger c_{j3\sigma_3} c_{i3\sigma_1} |\phi_0\rangle \quad (A7)$$

$$\sum_m (T^{pd})_{jm}^\dagger |\phi_{3i}^{sc,b}\rangle = - \sum_{ba} \sum_{lk} \sum_{\sigma_8 \sigma_6 \sigma_4 \sigma_3} \sum_{\sigma_2 \sigma_1} \frac{(t_{3b}^{jl})_{\sigma_8 \sigma_6} (t_{3a}^{ik})_{\sigma_6 \sigma_4} (t_{b3}^{lj})_{\sigma_4 \sigma_3} (t_{a3}^{ki})_{\sigma_2 \sigma_1}}{(\epsilon_{lb}^{pd} + \epsilon_{ka}^{pd} + U_p \delta_{kl}) \epsilon_{lb}^{pd}} \left(\frac{1}{\epsilon_{lb}^{pd}} + \frac{1}{\epsilon_{ka}^{pd}} \right) c_{j3\sigma_8}^\dagger c_{i3\sigma_6}^\dagger c_{j3\sigma_3} c_{i3\sigma_1} |\phi_0\rangle \quad (A8)$$

Processes in which the holes return to the ground state in reversed order have the intermediate state $|\phi_{3j}^{sc}\rangle$ in which Ir ion at site j and i are in the ground and excited states, respectively. This intermediate state is again a sum of two contributions which are taken to the ground state $|\phi_0\rangle$ upon acting with the second hopping Hamiltonian. The final state corresponds to Eqs. A7 and A8 upon exchanging $i \leftrightarrow j$ in the first and second matrix elements (i.e., those

returning the holes to their ground states) and the c^\dagger 's. Upon relabeling of spin indices these four contributions to the superexchange pathway from the simultaneous channel can be combined into a sum of two contributions, whose overlap with the ground state is

$$\begin{aligned} \langle \phi_0 | & \left(\sum_{ba} \sum_{lk} \sum_{\sigma_8 \sigma_6 \sigma_4 \sigma_3} \sum_{\sigma_2 \sigma_1} \frac{(t_{3a}^{jk})_{\sigma_8 \sigma_2} (t_{3b}^{il})_{\sigma_6 \sigma_4} (t_{b3}^{lj})_{\sigma_4 \sigma_3} (t_{a3}^{ki})_{\sigma_2 \sigma_1}}{\epsilon_{lb}^{pd} + \epsilon_{ka}^{pd} + U_p \delta_{kl}} \left(\frac{1}{\epsilon_{lb}^{pd}} + \frac{1}{\epsilon_{ka}^{pd}} \right)^2 c_{j3\sigma_8}^\dagger c_{i3\sigma_6}^\dagger c_{j3\sigma_3} c_{i3\sigma_1} \right. \\ & \left. + \sum_{ba} \sum_{lk} \sum_{\sigma_8 \sigma_6 \sigma_4 \sigma_3} \sum_{\sigma_2 \sigma_1} \frac{(t_{3a}^{ik})_{\sigma_8 \sigma_2} (t_{3b}^{jl})_{\sigma_6 \sigma_4} (t_{b3}^{lj})_{\sigma_4 \sigma_3} (t_{a3}^{ki})_{\sigma_2 \sigma_1}}{\epsilon_{lb}^{pd} + \epsilon_{ka}^{pd} + U_p \delta_{kl}} \left(\frac{1}{\epsilon_{lb}^{pd}} + \frac{1}{\epsilon_{ka}^{pd}} \right)^2 c_{i3\sigma_8}^\dagger c_{j3\sigma_6}^\dagger c_{j3\sigma_3} c_{i3\sigma_1} \right) | \phi_0 \rangle \end{aligned} \quad (A9)$$

Permuting some of the c, c^\dagger and applying identity Eq. 15, this can be summarized in the more compact form

$$\begin{aligned} \mathcal{H}_{i,j}^{(4sc)} = & \sum_{ba} \sum_{lk} \frac{1}{\epsilon_{lb}^{pd} + \epsilon_{ka}^{pd} + U_p \delta_{kl}} \left(\frac{1}{\epsilon_{lb}^{pd}} + \frac{1}{\epsilon_{ka}^{pd}} \right)^2 \text{tr} \left(t_{3b}^{il} t_{b3}^{lj} \left(\frac{1}{2} + \mathbf{S}_j \cdot \sigma \right) t_{3a}^{jk} t_{a3}^{ki} \left(\frac{1}{2} + \mathbf{S}_i \cdot \sigma \right) \right) \\ & + \sum_{ba} \sum_{lk} \frac{1}{\epsilon_{lb}^{pd} + \epsilon_{ka}^{pd} + U_p \delta_{kl}} \left(\frac{1}{\epsilon_{lb}^{pd}} + \frac{1}{\epsilon_{ka}^{pd}} \right)^2 \text{tr} \left(t_{3b}^{jl} t_{b3}^{lj} \left(\frac{1}{2} + \mathbf{S}_j \cdot \sigma \right) \right) \text{tr} \left(t_{3a}^{ik} t_{a3}^{ki} \left(\frac{1}{2} + \mathbf{S}_i \cdot \sigma \right) \right) \end{aligned} \quad (A10)$$

where the trace is again in spin-space. The second term as well as contributions from 1/2 in the first term lead to spin independent contributions. Neglecting these, we arrive at the effective Hamiltonian Eq. 28.

Appendix B: Traces over Pauli matrices

to find

Starting out from the expression

$$\begin{aligned} & \text{tr} ((A_1 + \mathbf{B}_1 \cdot \sigma)(\mathbf{S}_i \cdot \sigma)(A_2 + \mathbf{B}_2 \cdot \sigma)(\mathbf{S}_j \cdot \sigma)) \\ & = S_i^k S_j^l A_1 A_2 \text{tr} (\sigma^k \sigma^l) + S_i^k S_j^m A_1 B_2^l \text{tr} (\sigma^k \sigma^l \sigma^m) \\ & + S_i^l S_j^m A_2 B_1^k \text{tr} (\sigma^k \sigma^l \sigma^m) + S_i^k S_j^m B_1^l B_2^k \text{tr} (\sigma^k \sigma^l \sigma^m \sigma^n) \end{aligned} \quad (B1)$$

we use the identities

$$\text{tr} (\sigma^k \sigma^l) = 2\delta_{kl} \quad (B2)$$

$$\text{tr} (\sigma^k \sigma^l \sigma^m) = 2i\epsilon_{klm} \quad (B3)$$

$$\text{tr} (\sigma^k \sigma^l \sigma^m \sigma^n) = 2(\delta_{kl}\delta_{mn} - \delta_{km}\delta_{ln} + \delta_{kn}\delta_{lm}) \quad (B4)$$

$$\begin{aligned} & \frac{1}{2} \text{tr} ((A_1 + \mathbf{B}_1 \cdot \sigma)(\mathbf{S}_i \cdot \sigma)(A_2 + \mathbf{B}_2 \cdot \sigma)(\mathbf{S}_j \cdot \sigma)) \\ & = A_1 A_2 \mathbf{S}_i \cdot \mathbf{S}_j + i(A_2 \mathbf{B}_1 - A_1 \mathbf{B}_2) \cdot (\mathbf{S}_i \times \mathbf{S}_j) \\ & + \mathbf{S}_i \cdot \left(\overleftarrow{\mathbf{B}_1} \overrightarrow{\mathbf{B}_2} + \overleftarrow{\mathbf{B}_2} \overrightarrow{\mathbf{B}_1} - \mathbf{B}_1 \cdot \mathbf{B}_2 \mathbb{1} \right) \cdot \mathbf{S}_j \end{aligned} \quad (B5)$$

- ¹ Y. Okamoto, M. Nohara, H. Aruga-Katori and H. Takagi, Phys. Rev. Lett. **99**, 137207 (2007).
- ² P. A. Lee, Science **321**, 1306 (2008).
- ³ G. Chen and L. Balents, Phys. Rev. B **78**, 094403 (2008).
- ⁴ M. R. Norman and T. Micklitz, Phys. Rev. B **81**, 024428 (2010).
- ⁵ T. Yildirim, A. B. Harris, A. Aharony and O. Entin-Wohlmann, Phys. Rev. B **52**, 10239 (1995).
- ⁶ O. Entin-Wohlmann, A. B. Harris and A. Aharony, Phys. Rev. B **53**, 11661 (1996).
- ⁷ W. Koshibae, Y. Ohta and S. Maekawa, Phys. Rev. B **47**, 3391 (1993).
- ⁸ W. Koshibae, Y. Ohta and S. Maekawa, Phys. Rev. B **50**, 3767 (1994).
- ⁹ L. F. Mattheiss, Phys. Rev. B **13**, 2433 (1976).
- ¹⁰ J. C. Slater and G. F. Koster, Phys. Rev. **94**, 1498 (1954).

- ¹¹ M. D. Jones and R. C. Albers, Phys. Rev. B **79**, 045107 (2009).
- ¹² W. H. Press, B. P. Flannery, S. A. Teukolsky and W. T. Vetterling, *Numerical Recipes* (Cambridge University Press, Cambridge, 1989).
- ¹³ S. J. Moon, H. Jin, K. W. Kim, W. S. Choi, Y. S. Lee, J. Yu, G. Cao, A. Sumi, H. Funakubo, C. Bernhard and T. W. Noh, Phys. Rev. Lett. **101**, 226402 (2008).
- ¹⁴ G. Jackeli and G. Khaliullin, Phys. Rev. Lett. **102**, 017205 (2009).
- ¹⁵ A. Shitade, H. Katsura, J. Kunes, X.-L. Qi, S.-C. Zhang and N. Nagaosa, Phys. Rev. Lett. **102**, 256403 (2009).
- ¹⁶ D. Podolsky and Y. B. Kim, arXiv:0909.4546.
- ¹⁷ P. A. Lee, N. Nagaosa and X.-G. Wen, Rev. Mod. Phys. **78**, 17 (2006).